Silicon Solid Electrolyte Interphase (SEI) of Lithium Ion Battery Characterized by Microscopy and Spectroscopy

ARTICLE *in* THE JOURNAL OF PHYSICAL CHEMISTRY C · JUNE 2013

Impact Factor: 4.77 · DOI: 10.1021/jp404155y

5 AUTHORS, INCLUDING:

Mengyun Nie
Dalhousie University
24 PUBLICATIONS **201** CITATIONS
SEE PROFILE

Daniel P. Abraham
Argonne National Laboratory
148 PUBLICATIONS **3,258** CITATIONS
SEE PROFILE

Yanjing Chen
29 PUBLICATIONS **393** CITATIONS
SEE PROFILE

THE JOURNAL OF PHYSICAL CHEMISTRY C

Article

pubs.acs.org/JPCC

Silicon Solid Electrolyte Interphase (SEI) of Lithium Ion Battery Characterized by Microscopy and Spectroscopy

Mengyun Nie,[†] Daniel P. Abraham,[‡] Yanjing Chen,[†] Arijit Bose,[†] and Brett L. Lucht*[,†]

[†]University of Rhode Island, Kingston, Rhode Island 02881, United States

[‡]Argonne National Laboratory, Argonne, Illinois 60439, United States

ABSTRACT: The surface reactions of electrolytes with a silicon anode in lithium ion cells have been investigated. The investigation utilizes two novel techniques that are enabled by the use of binder-free silicon (BF-Si) nanoparticle anodes. The first method, transmission electron microscopy with energy dispersive X-ray spectroscopy, allows straightforward analysis of the BF-Si solid electrolyte interphase (SEI). The second method utilizes multi-nuclear magnetic resonance spectroscopy of D_2O extracts from the cycled anodes. The TEM and NMR data are complemented by XPS and FTIR data, which are routinely used for SEI studies. Coin cells (BF-Si/Li) were cycled in electrolytes containing $LiPF_6$ salt and ethylene carbonate or fluoroethylene carbonate solvent. Capacity retention was significantly better for cells cycled with $LiPF_6$/FEC electrolyte than for cells cycled with $LiPF_6$/EC electrolyte. Our unique combination of techniques establishes that for $LiPF_6$/EC electrolyte the BF-Si SEI continuously grows during the first 20 cycles and the SEI becomes integrated with the BF-Si nanoparticles. The SEI predominantly contains lithium ethylene dicarbonate, LiF, and Li_xSiO_y. BF-Si electrodes cycled with $LiPF_6$/FEC electrolyte have a different behavior; the BF-Si nanoparticles remain relatively distinct from the SEI. The SEI predominantly contains LiF, Li_xSiO_y, and an insoluble polymeric species.

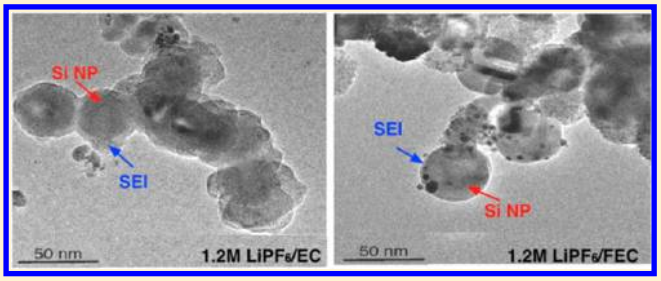

INTRODUCTION

There has been significant interest in the development of lithium ion batteries due to the high-energy density of these secondary batteries. However, meeting the requirements of electric vehicles (EVs) requires the development of anode and cathode materials with higher energy density than the anode and cathode materials used in traditional lithium ion batteries. Silicon is one of the most promising candidates for an anode material in LIBs due to the high theoretical capacity, 3580 mAh/g, when fully lithiated.[1] This theoretical capacity is ~10 times that of commercial graphite (372 mAh/g) currently used in lithium ion batteries. However the silicon electrodes have a very large volume expansion (300−400%) during lithiation, resulting in large stresses, mechanical damage, and surface area changes.[2,3] The problems associated with the large volumetric changes have prompted the design and application of nanostructured silicon materials.[4,5] It is well known that during the first charging cycles a solid electrolyte interphase (SEI) is generated on the surface of the graphite anode in lithium ion batteries. Significant research has been conducted on the structure and composition of the graphite SEI.[6,7] The structure and stability of the graphite SEI has been reported to be dependent on the composition of the electrolyte, salt, solvent, and additives.[8,9] A related SEI has been reported to be generated on the surface of silicon electrodes in lithium ion batteries.[10] However, the instability of the SEI on silicon electrodes is a significant problem, leading to poor capacity retention.

Analysis of the SEI generated on silicon anodes has been conducted by several research groups with standard $LiPF_6$/ethylene carbonate (EC)-based electrolytes. One investigation of SEI formation on silicon nanoparticles was conducted via a combination of hard and soft X-ray photoelectron spectroscopy (XPS), suggesting that the SEI on the silicon electrodes at the electrolyte interface is similar to the SEI formed on carbonaceous electrodes and is dominated by lithium alkyl carbonates, while the SEI at the silicon interface is dominated by the conversion of the surface SiO_2 layer to Li_xSiO_y.[11] Another investigation of SEI formation on silicon in EC-based electrolytes was conducted via a combination of XPS, IR, and Raman spectroscopy. The analysis was conducted as a function of electrochemical potential during the first charge and revealed an SEI composed primarily of LiF, Li_xPF_y, lithium alkyl carbonates, and lithiated fluorosilicates Li_xSiF_y.[12] In addition, the presence of ionic species including LiF or Li_2CO_3 at the silicon anode electrolyte interface was supported by ex situ ^{7}Li MAS NMR spectra.[13]

To improve the cycling behavior of silicon anodes in lithium ion batteries, we have modified the electrolyte formulation via the addition of reactive additives or cosolvents designed to generate a more stable SEI. One of the most frequently investigated additives is fluoroethylene carbonate (FEC). The

Received: April 26, 2013
Revised: June 7, 2013
Published: June 7, 2013

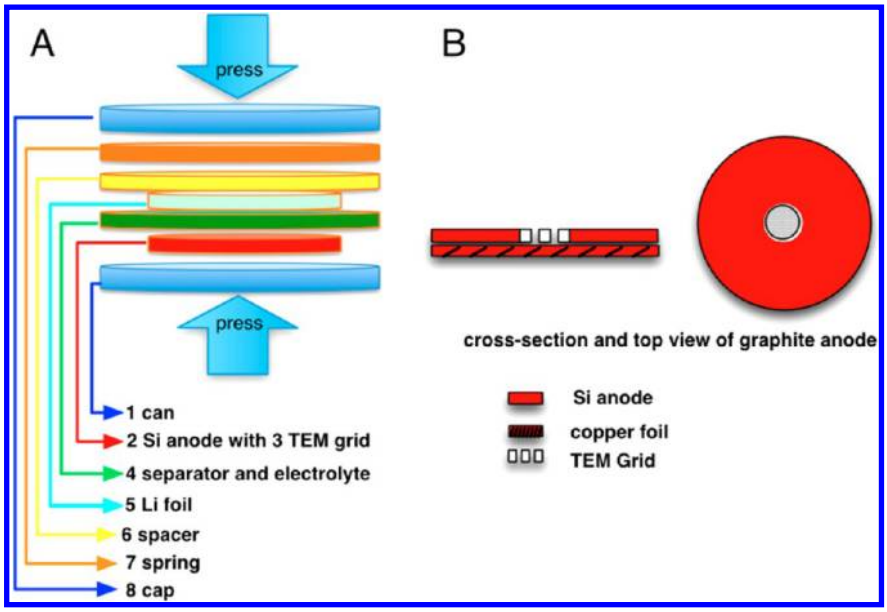

Figure 1. Schematic diagram and picture showing (A) the assembly of a Li/BF-Si half-cell and (B) TEM-grid embedded BF-Si electrode.

addition of FEC has been investigated in low concentrations (1−5%) as an additive and in high concentrations (10−50%) as a cosolvent in $LiPF_6$/carbonate electrolytes. The addition of FEC has been reported to significantly improve the capacity retention of many silicon electrodes.[14] Surface analysis of silicon electrodes, via SEM, XPS, and IR, cycled with electrolyte containing a low concentration of FEC (3 wt %), suggests that the SEI contains LiF, lithium alkyl carbonates, and fluorinated silicon species (Si−F) and has many similarities to the SEI generated with $LiPF_6$ in carbonates without FEC.[15,16] Investigation of the surface of silicon anodes cycled with higher concentrations of FEC provided different results. Analysis of the electrode surface via a combination of XPS, TEM, TOF-SIMS, and IR spectroscopy suggests that the surface has a high concentration of LiF and a polymer that may be a polyalkene or polycarbonate.[17,18] However lithium alkyl carbonates are also observed due to the presence of EC and dialkyl carbonates in the electrolyte. The presence of FEC is believed to generate a thinner SEI, with a lower impedance, on the silicon surface.[17,19] However, even in the presence of FEC, the SEI on the silicon anode is not as stable as the SEI on graphite anodes. The SEI instability contributes to the poor cycling performance of silicon anodes. Therefore, a better understanding of the SEI on silicon anodes in EC- and FEC-based electrolytes is necessary.

We have developed novel binder-free silicon (BF-Si) nanoparticle electrodes and investigated the cycling performance in $LiPF_6$/EC and $LiPF_6$/FEC electrolytes. The absence of binder and presence of a single solvent electrolyte simplifies the analysis of the SEI components. After cycling, ex situ analysis of the silicon electrodes has been conducted via a combination of TEM, solution NMR spectroscopy of electrode extracts, FT-IR, and XPS. The specially designed TEM experiment allows direct imaging of the silicon nanoparticles after cycling, while analysis of the D_2O extracts provides the molecular structure of the SEI components.[20] The analysis provides information about the components of the SEI resulting from electrolyte (salt and solvent) decomposition on silicon anodes and insights into the difference in cycling performance for electrolytes containing FEC.

EXPERIMENTAL SECTION

Preparation of Binder-Free Silicon Electrodes and Coin Cells Fabrication. BF-Si electrodes were prepared by electrophoretic deposition (EPD) methods in a similar manner to our previously reported preparation of binder-free graphite electrodes.[21,22] The EPD bath was prepared with silicon nanoparticles (~50 nm, Alfa Aesar) dissolved in acetonitrile (anhydrous, Fisher). Utilizing this method results in the preparation of electrodes without polymer binders (PVDF, CMC, SBR, etc.) or conductive carbon. The electrodes are exclusively composed of silicon nanoparticles with a theoretical capacity of ~3580 mAh/g.[1] BF-Si electrodes were coated on copper foil with a surface density of ~0.37 mg/cm^2. The BF-Si electrodes were vacuum-dried for 24 h at 120 °C. Coin cells (CR2032) were fabricated with BF-Si electrodes, polypropylene separator (Celgard 3501), and lithium foil in a high purity Ar-filled glovebox. Two different electrolytes were used: 1.2 M $LiPF_6$ in EC (BASF) and 1.2 M $LiPF_6$ in FEC (BASF). Each coin cell contains 30 μL of electrolyte.

Special coin cells, containing BF-Si electrodes with copper TEM grids (Figure 1) were assembled.[20] Silicon was removed from the center of the BF-Si electrode to allow placement of the copper TEM grid. During cell construction some of the silicon nanoparticles shifted from the BF-Si electrode and adhered to the copper TEM grid, enabling TEM visualization of cycled Si particles. Cell assembly was conducted in an Ar-atmosphere glovebox (<1 ppm H_2O). TEM images of fresh silicon nanoparticles were acquired by dispersing silicon nanoparticles on TEM grids with a polymer coating to allow adhesion of the nanoparticles to the grid.

Electrochemical Cycling. Coin cells undergo a constant-current charge and discharge between 2.0 to 0.05 V on a ARBIN BT 2000 cycler with a current density of ~50 μA/cm^2, which is an approximately C/20 rate. The cells were cycled with the following procedures: first cycle at C/20, second cycle at C/10, and remaining cycles at C/5 at 25 °C. Cells cycled comparably with and without the integrated TEM grids.

XPS, FTIR, and NMR Analysis. XPS of BF-Si electrodes was conducted on a PHI 5500 system using Al K_α radiation source ($h\nu$ = 1486 eV). The binding energies of all elements

dx.doi.org/10.1021/jp404155y | J. Phys. Chem. C 2013, 117, 13403−13412

were calibrated based on the C−H binding energy at 285 eV. The spectra were analyzed and fitted by Multipack 6.1 and XPS peak software (version 4.1). Line syntheses of elemental spectra were conducted using Gaussian−Lorentzian (70:30) curve fitting. Element concentration was calculated based on the equation: $C_x = (I_x/S_x)/(\sum I_i/S_i)$, where I_x is the intensity of the relative element and S_i is the sensitivity number of the element.[23] Scanning electron microscopy was conducted on a JEOL-5900 SEM. FTIR-ATR spectra were acquired on a Bruker-2700 apparatus with Ge crystal detector; the data were collected in an Ar-purged chamber. All NMR samples were prepared via extraction from cycled BF-Si electrodes by D_2O in an Ar-filled glovebox; the BF-Si electrodes were rinsed with anhydrous DMC to remove residual electrolyte and dried overnight under vacuum prior to D_2O extraction. Multinuclear NMR analyses were conducted on a Bruker Avance III 300 MHz NMR spectrometer.

RESULTS

Electrochemical Cycling. The first cycle plots for $LiPF_6$/EC and $LiPF_6$/FEC electrolytes have similar lithiation capacities (~3000 mAh/g) and delithiation capacities (~1800 mAh/g) (Figure 2a). Thus, both electrolytes also have large first-cycle irreversible capacity, 38 and 36% for $LiPF_6$/EC and $LiPF_6$/FEC, respectively. The first cycle discharge capacity and cycling efficiency are in agreement with previous reports.[24,25] The capacity retention for BF-Si electrodes cycled for 20 cycles with $LiPF_6$/EC and $LiPF_6$/FEC electrolytes is depicted in Figure 2b. Because of the nature of binder-free electrodes and silicon anode materials, the electrodes suffer more rapid capacity fading than other silicon electrodes. However, better capacity retention (~1000 mAh/g after 20 cycles) and more stable cycling efficiency (~98%) are observed for cells cycled with the $LiPF_6$/FEC electrolyte.

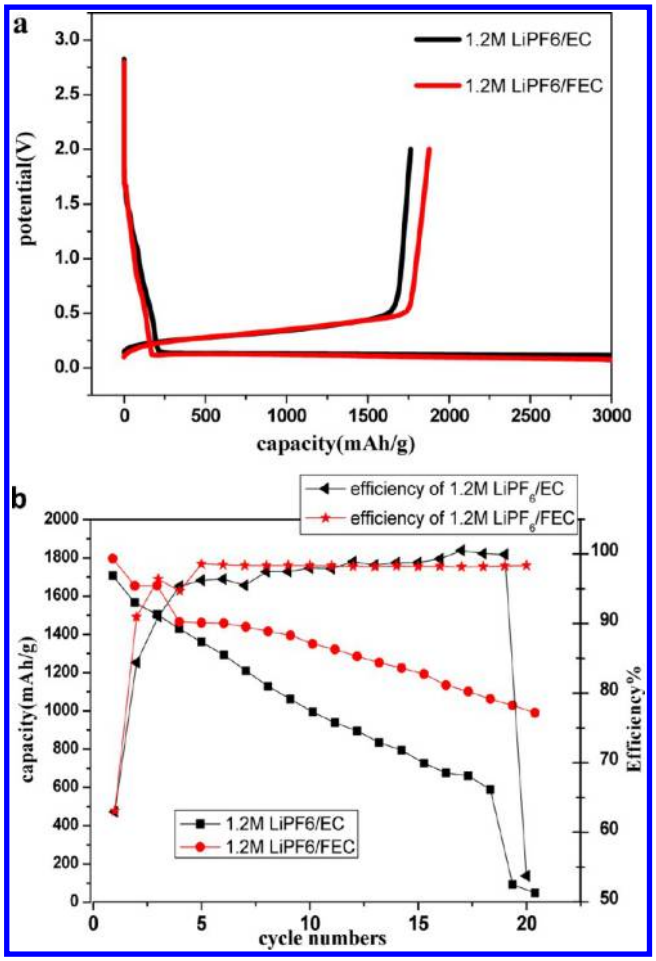

Figure 2. (a) First cycle charge/discharge profiles of BF-Si electrodes half cells with two electrolytes. (b) Cycling performance of EC and FEC-containing electrolytes in BF-Si cells at 20 cycles.

Good reversible cycling of graphite or silicon anodes in lithium ion batteries requires the generation of a stable SEI.[26,27] Thus the differences in cycling performance between EC and FEC suggest that there may be differences in the SEI generated in the presence of different solvents. To develop a better understanding of the different cycling behavior, the $LiPF_6$/EC and $LiPF_6$/FEC containing cells were disassembled, and ex situ analysis of the BF-Si electrodes was conducted after the 1st, 5th, and 20th cycles.

TEM Analysis of BF-Si Electrode. Integration of TEM grids into the BF-Si anode allows the acquisition of images of cycled silicon nanoparticles directly from cells after cycling. The morphology of BF-Si anode particles has been monitored after the 1st, 5th, and 20th cycle. The morphology of BF-Si anodes cycled with $LiPF_6$/EC electrolyte compared with fresh BF-Si anode nanoparticles is depicted in Figure 3, while the elemental concentrations of the surface, as determined by EDX, are provided in the Figure 3 insets. After one cycle, the sharp edges of the fresh silicon nanoparticles are converted to a rough inhomogeneous layer consistent with the generation of an SEI. However, the individual Si nanoparticles remain discrete. EDX analysis indicates the presence of C, O, F, and P (5.9, 9.6, 0.9, and 0.5%, respectively), consistent with the deposition of electrolyte decomposition products. After five cycles, the Si nanoparticles are covered and connected by a thick SEI, and the silicon particles are no longer discrete (Figure 3c). The surface EDX concentrations of C, O, F, and P (13.2, 18.1, 1.5, and 0.5, respectively) are higher and consistent with a thicker SEI. The integration of the SEI with the BF-Si nanoparticles is more apparent after 20 cycles. The C and O concentrations are comparable to the concentration of Si (26.2, 33.4, and 36.2%, respectively), suggesting a very high concentration of electrolyte decomposition products on the surface of the BF-Si nanoparticles and incorporation of Si containing species into the SEI. The repeated volume expansion and contraction of the nanoparticle leads to significant increases in the concentration of electrolyte decomposition products and results in significant change to the silicon nanoparticles.[28,29]

Analysis of the BF-Si electrode cycled with the $LiPF_6$/FEC electrolyte suggests different and less severe morphological changes to the nanoparticles (Figure 4). After the first cycle, the BF-Si particles retain a spherical shape and have clear edges. A thinner SEI is observed with grainy particles (5−10 nm) on the surface of the silicon nanoparticles. The elemental concentrations of C and O are similar to those observed for BF-Si cycled with $LiPF_6$/EC electrolyte, but the concentration of F is much higher (5.2% compared with 0.9% for the electrode cycled with $LiPF_6$/EC). After additional cycling, the SEI becomes thicker and very grainy. However, the Si nanoparticles remain largely intact and the SEI and Si nanoparticles appear more distinctly separate than that observed for BF-Si cycled with $LiPF_6$/EC electrolyte. Thus the deposition of the electrolyte decomposition products appears to be occurring on the surface of the Si nanoparticles with the $LiPF_6$/FEC

dx.doi.org/10.1021/jp404155y | J. Phys. Chem. C 2013, 117, 13403−13412

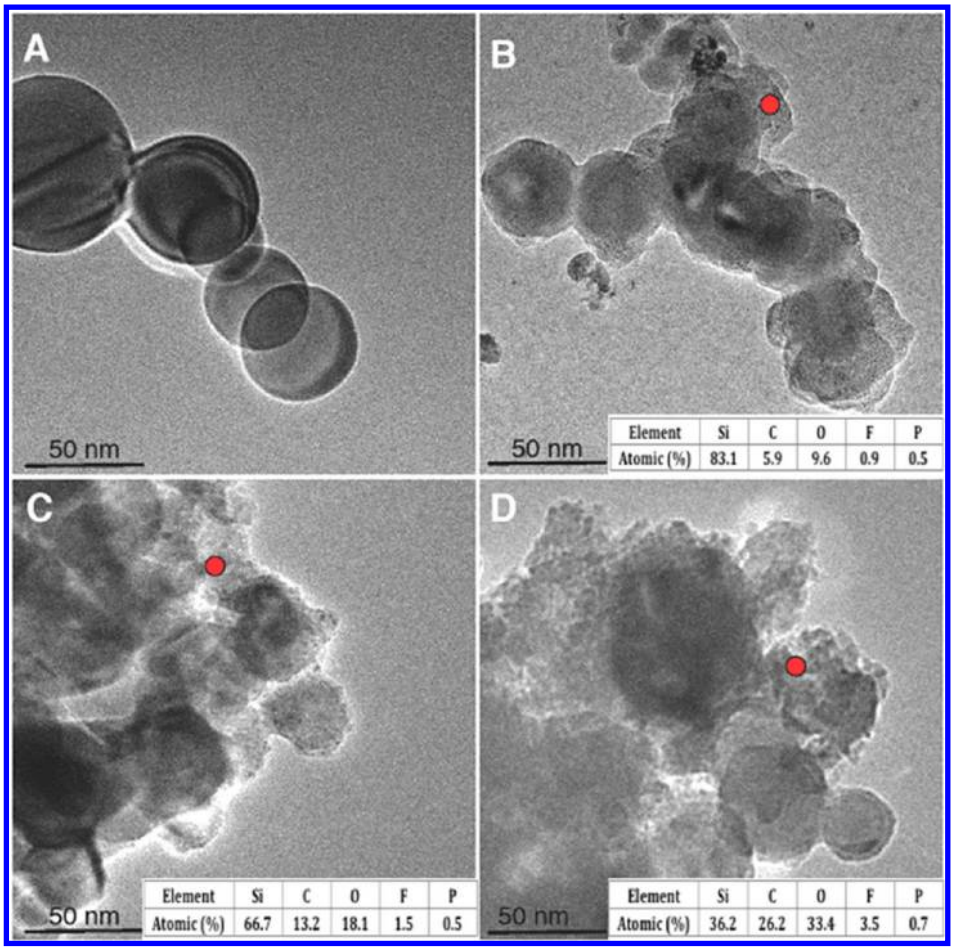

Figure 3. TEM images of BF-Si electrodes cycled with 1.2 M $LiPF_6$/EC (right): (A) Fresh BF-Si, (B) BF-Si after 1st cycle, (C) BF-Si with 5th cycle, and (D) BF-Si after 20th cycle.

electrolyte. The composition of the SEI generated from the $LiPF_6$/FEC electrolyte is also quite different than the SEI generated from the $LiPF_6$/EC electrolyte. Analysis of the elemental concentration at the surface with EDX after 20 cycles suggests that the SEI generated from $LiPF_6$/FEC has a much higher concentration of F than the SEI generated from $LiPF_6$/EC, 32.8 and 3.5%, respectively.

The cycled BF-Si electrodes were also analyzed by TEM after extraction with D_2O (Figure 5). The cycled BF-Si electrodes were extracted with D_2O to allow the characterization of SEI components via solution NMR spectroscopy, as described below.[20] After extraction, the residual silicon nanoparticles were deposited onto a TEM grid and vacuum-dried. The silicon nanoparticles cycled with EC or FEC have very different morphology after D_2O extraction. The thick integrated SEI formed on the BF-Si electrode after cycling with $LiPF_6$/EC is no longer observed. Some distinct silicon nanoparticles are observed, but most of the material is agglomerated into fused particles. Analysis of the particles by EDX reveals a significant decrease in the concentration of C and F (14.6 and 0.7%, respectively) after extraction, suggesting that most of the C and F containing species are dissolved in the D_2O. The residual nanoparticles are dominated by Si and O, 26.1 and 58.5%, respectively, consistent with the presence of SiO_x. The silicon nanoparticles cycled with $LiPF_6$/FEC are also significantly modified upon D_2O extraction. Analysis of the silicon nanoparticles by EDX reveals a large decrease in the concentration of F (32.8 to 0.3%) and a large increase in the concentration of C (26.5 to 70.5%), suggesting that most of the F-containing species are soluble in D_2O, while most of the C containing species are D_2O insoluble. Thus the C containing SEI components generated from $LiPF_6$/EC and $LiPF_6$/FEC have significantly different structures and properties.

XPS Analysis of BF-Si Electrodes. The XPS spectra of BF-Si electrodes extracted from cells cycled with $LiPF_6$/EC electrolyte after the 1st, 5th, and 20th cycle are presented in Figure 6, and the elemental concentrations are summarized in Table 1. The absence of binder in the BF-Si electrodes allows more straightforward analysis of the SEI. The spectra suggest changes to the electrodes surface as a result of cycling. The fresh BF-Si electrode is dominated by Si and O due to the presence of SiO_2 on the surface of the nanoparticles and contains a weak C peak associated with universal carbon contamination. Upon cycling with $LiPF_6$/EC electrolyte, the concentration of Si decreases significantly; the concentration of O also decreases, but the concentrations of C and F increase. The largest changes are observed after the first cycle, but the elemental concentrations continue to have small fluctuations with increased cycling, which suggests that the SEI continues to evolve.

The element spectra of the fresh BF-Si electrode contain two clearly separated peaks in the Si 2p spectrum characteristic of SiO_2 (103.5 eV) and Si (99.5 eV). Upon cycling, the two strong peaks are converted to a weak broad peak centered at ~102 eV,

dx.doi.org/10.1021/jp404155y | J. Phys. Chem. C 2013, 117, 13403−13412

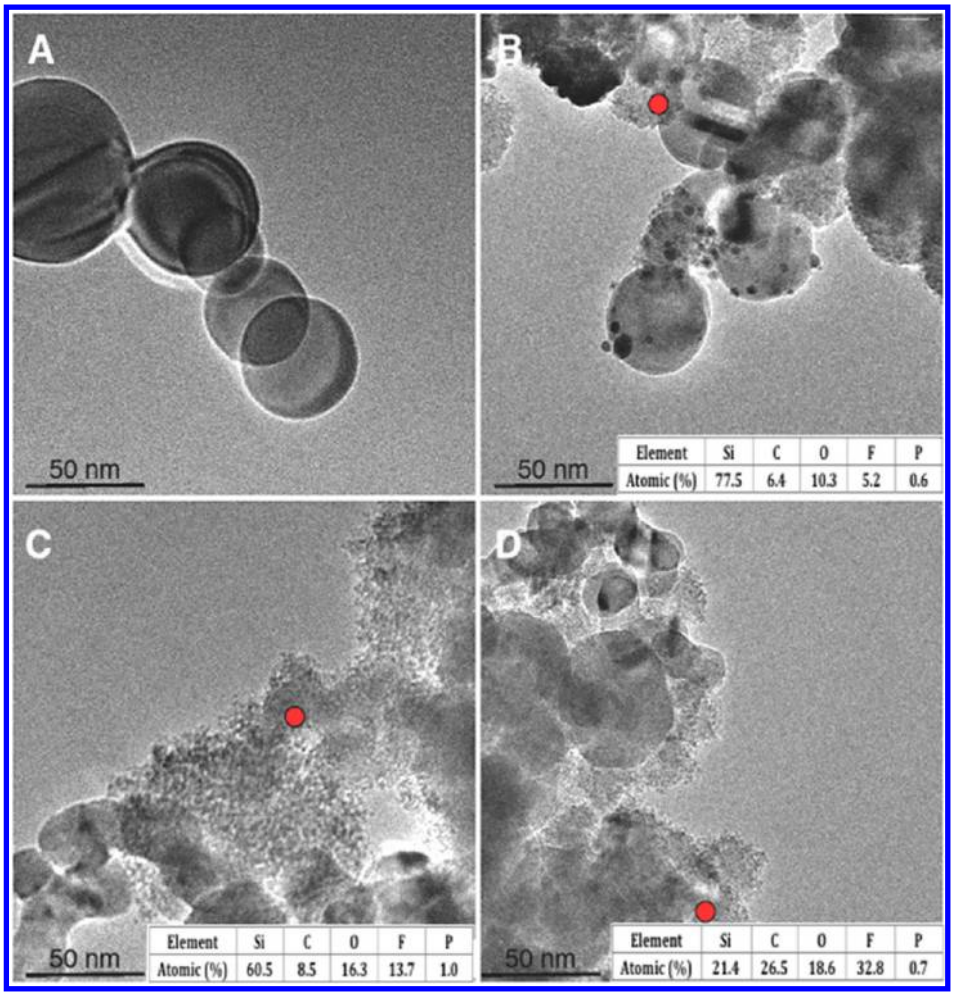

Figure 4. TEM images of BF-Si electrodes cycled with 1.2 M $LiPF_6$/FEC (right): (A) Fresh BF-Si, (B) BF-Si after 1st cycle, (C) BF-Si with 5th cycle, and (D) BF-Si after 20th cycle.

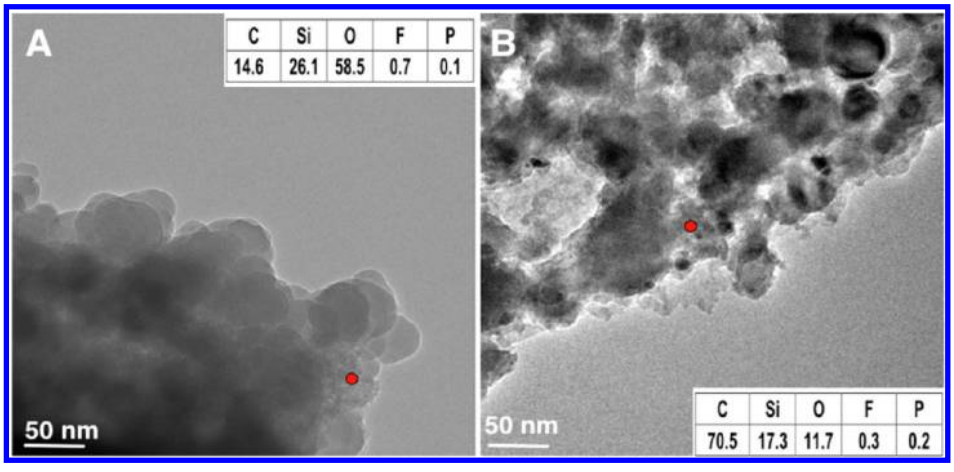

Figure 5. TEM images of BF-Si electrodes after 20 cycles, followed by D_2O extraction. (Left) 1.2 M $LiPF_6$/EC and (Right) 1.2 M $LiPF_6$/FEC.

which is assigned to Li_xSiO_y.[11] For the fresh electrode the major C1s peak at 285 eV is consistent with alkane species and the universal hydrocarbon contamination. Upon cycling, new C1s peaks are observed at 286.5 and 290 eV, consistent with the presence of species containing C−O and O−(C═O)−O, respectively. A single broad peak is observed in the O1s spectra, consistent with the presence of C−O and O−(C═O)−O containing species at 533−534 and 532−533 eV, respectively. The peaks observed in the C1s and O1s spectra are consistent with the presence of LEDC, from the reduction of EC. The F1s spectrum contains a single peak at 685 eV supporting the presence of LiF.[16] The XPS results are similar to those previously reported for thin film silicon, silicon nanowires, and silicon nanoparticles and consistent with the generation of an SEI composed of LEDC, LiF, and some Li_xSiO_y.[11,17,18] The concentration of silicon is low, suggesting that the SEI is

dx.doi.org/10.1021/jp404155y | J. Phys. Chem. C 2013, 117, 13403−13412

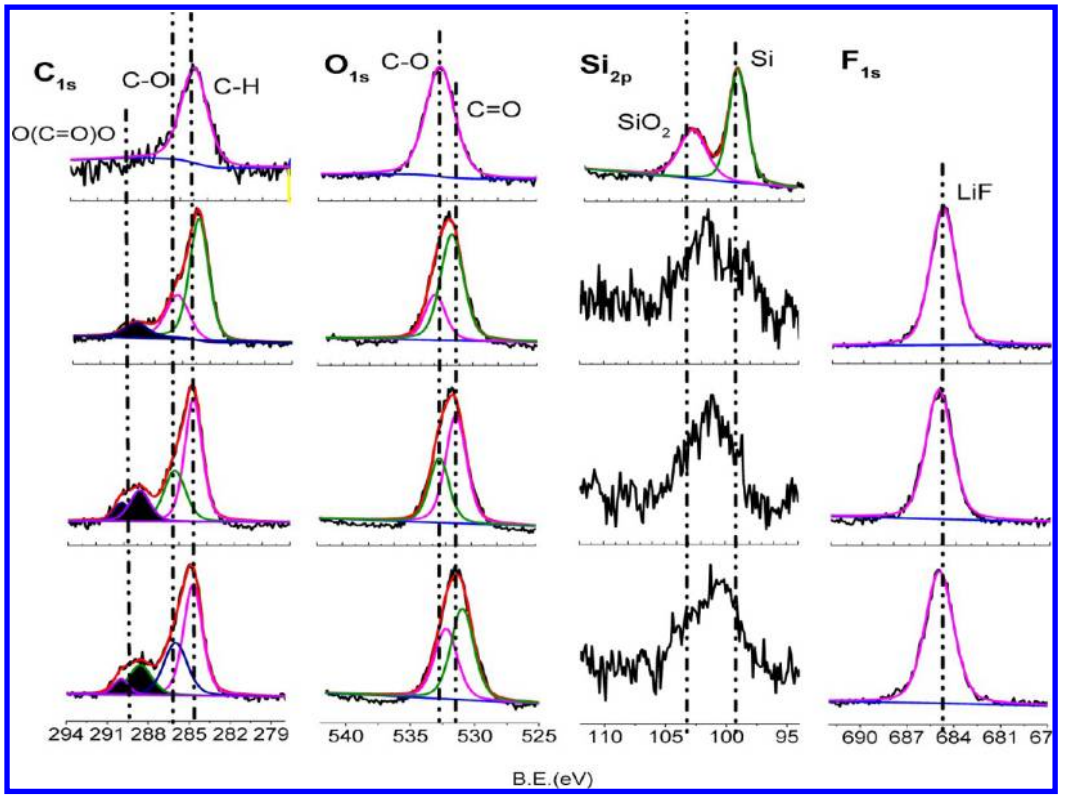

Figure 6. XPS spectra of BF-Si electrode cycled with EC-electrolyte from top: fresh electrode, 1st cycle, 5th cycle, and 20th cycle.

Table 1. Elemental Concentration on Fresh and Cycled BF-Si Electrodes for Different Cycle Numbers in EC-Electrolyte

element	C	O	Si	F
fresh	19.0	45.7	35.3	
1st	31.6	33.4	8.3	26.7
5th	36.1	35.9	4.6	23.4
20th	40.1	35.7	3.5	20.7

primarily composed of electrolyte reduction products and is similar to that observed on graphite electrodes.[20]

The XPS element spectra of BF-Si electrodes extracted from cells cycled with the $LiPF_6$/FEC electrolyte are provided in Figure 7, and the element concentrations are summarized in Table 2. Upon cycling with $LiPF_6$/FEC electrolyte the concentrations of Si and O decrease significantly while the concentrations of C and F increase, consistent with the generation of an SEI. Concentrations of Si, C, O, and F for BF-Si electrodes extracted after one cycle with $LiPF_6$/FEC electrolyte are similar to BF-Si electrodes extracted after one cycle with $LiPF_6$/EC electrolyte. However, upon additional cycling the concentration of F is significantly higher while the concentration of O is significantly lower for cells cycled with $LiPF_6$/FEC compared with cells cycled with $LiPF_6$/EC electrolyte, consistent with a change in the SEI structure.

The element spectra of the BF-Si electrode extracted from a cell after one cycle with $LiPF_6$/FEC contain two peaks in the Si2p spectrum at 99.5 and 103.5 eV, characteristic of Si and SiO_2, respectively. However, after 20 cycles the peaks for Si and SiO_2 are diminished and a peak at ∼102 eV is observed consistent with the formation of Li_xSiO_y.[11] The results are similar to those observed for BF-Si electrodes cycled with $LiPF_6$/EC electrolyte, although a larger number of cycles is required to bring about comparable changes. The other element spectra (C, O, and F) are changed significantly after the first cycle, but increased cycling results in only small changes. The C1s spectra contain three peaks at 285, 286.5, and 290 eV, characteristic of C−H, CH_2−O, and O−(C═O)−O containing species, and are similar to the C1s spectra of BF-Si electrodes cycled with $LiPF_6$/EC electrolytes, although the peaks characteristic of O−(C═O)−O containing species are weaker for electrodes cycled with the $LiPF_6$/FEC electrolyte. The O1s spectra contain a broad peak centered at ∼533 eV consistent with the presence of O−(C═O*)−O (532.5 eV) and O−(C═O)−O* (533.5 eV) containing species.[15] The F1s spectra contain a dominant peak for LiF at 685 eV and a small peak at 687 eV, suggesting the presence of $Li_xPF_yO_z$ or residual $LiPF_6$. The P2p XPS spectra are not included because of weak signal intensities. The XPS results support the TEM-EDX results, suggesting that the SEI is composed of LiF, Li_xSiO_y, and a polymeric species containing C−O and O−(C═O)−O bonds.[17,18] The concentration of LiF is much higher in the SEI generated from $LiPF_6$ in FEC than the SEI generated from $LiPF_6$ in EC.

FTIR Analysis of BF-Si Electrodes. FTIR spectra were collected from BF-Si electrodes extracted from cells cycled with $LiPF_6$/EC electrolyte after the 1st, 5th, and 20th cycles, respectively (Figure 8a). The fresh electrodes contain a broad absorbance with peaks at 1290 and 1120 cm^{-1} due to the Si−O functional group on the surface of the Si nanoparticles of the BF-Si electrodes. The IR spectrum of BF-Si electrode after the first cycle contains more absorption peaks located at 1652, 1416, 1305, 1145, and 870 cm^{-1}, characteristic of LEDC, as previously reported,[30] along with overlapping absorptions associated with Li_2CO_3 at 1420 cm^{-1}, O−Si−O at 1070 cm^{-1}, and residual $LiPF_6$ at 870 cm^{-1}. Continued cycling results in increases in the intensity of the peaks associated with LEDC, and decreases in the intensity of the Li_2CO_3 and O−Si−O

dx.doi.org/10.1021/jp404155y | J. Phys. Chem. C 2013, 117, 13403−13412

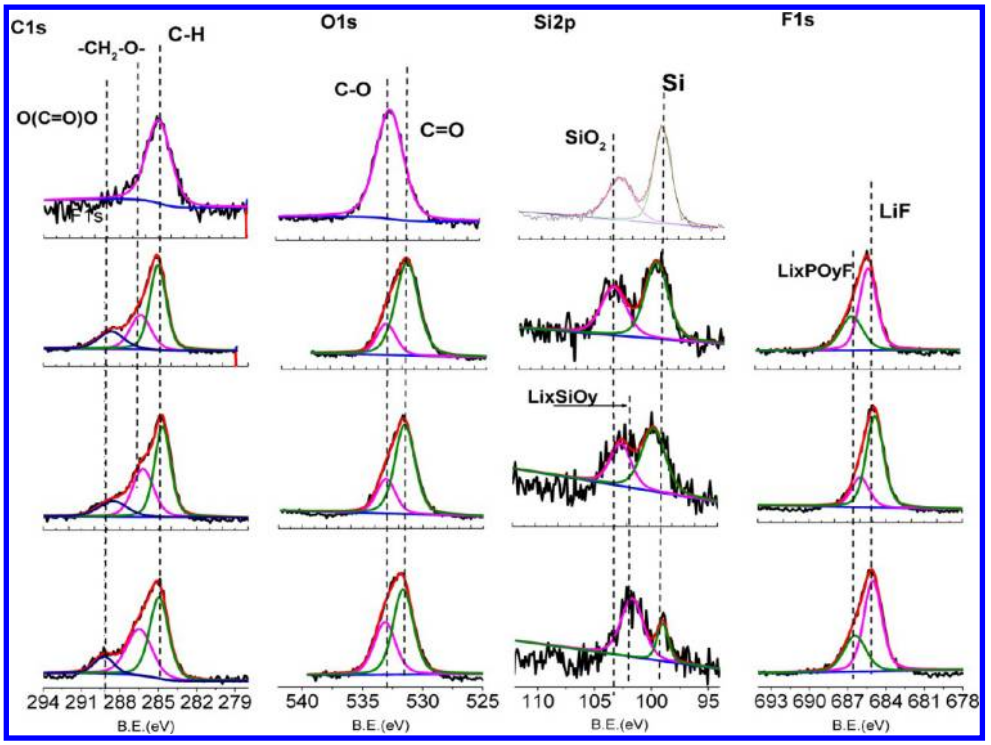

Figure 7. XPS spectra of BF-Si electrode cycled with FEC-electrolyte from top: fresh electrode, 1st cycle, 5th cycle, and 20th cycle.

Table 2. Elemental Concentration on Cycled BF-Si Electrodes for Different Cycle Numbers in FEC-Electrolyte

element	C	O	Si	F
fresh	19.0	45.7	35.3	
1st	32.7	28.7	15.2	23.4
5th	35.5	29.7	6.5	28.3
20th	35.8	29.5	5.3	29.4

absorptions consist of an increase in the concentration of LEDC with increased cycling and the generation of a thicker SEI. Other species may be present on the surface in low concentration. However, weak intensity and overlap of absorptions prevent further characterization.

A similar trend is observed for the IR spectra of BF-Si electrodes extracted from cells cycled with $LiPF_6$/FEC electrolyte (Figure 8b). Upon cycling the peaks characteristic of Si−O bonds at 1290 and 1120 cm^{-1} are diminished, consistent with the deposition of electrolyte decomposition products on the surface. The spectrum of the BF-Si electrode after one cycle contains weak absorption bands at: 1640, 1450, 1090, and 870 cm^{-1}. The strong absorption at 870 cm^{-1} is from residual $LiPF_6$.[22] Additional cycling of the BF-Si electrodes with $LiPF_6$/FEC electrolyte results in an increase in the intensity of the absorptions observed after one cycle, 1640, 1450, 1090

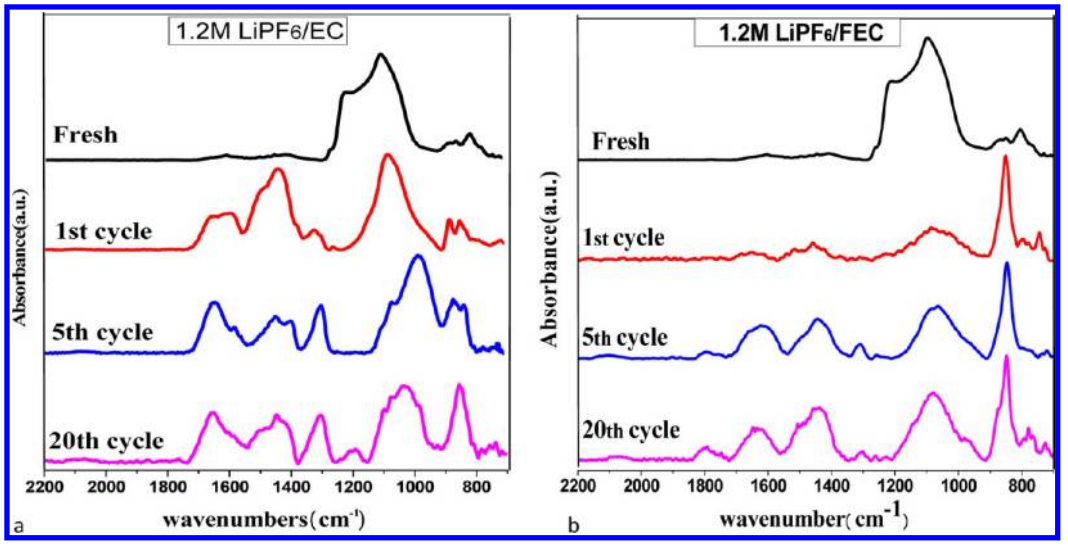

Figure 8. (a) IR spectra of BF-Si electrodes cycled with EC-electrolyte from top: fresh electrode, 1st, 5th, and 20th cycles. (b) BF-Si electrodes cycled with FEC-electrolyte from top: 1st, 5th, and 20th cycles.

dx.doi.org/10.1021/jp404155y | J. Phys. Chem. C 2013, 117, 13403−13412

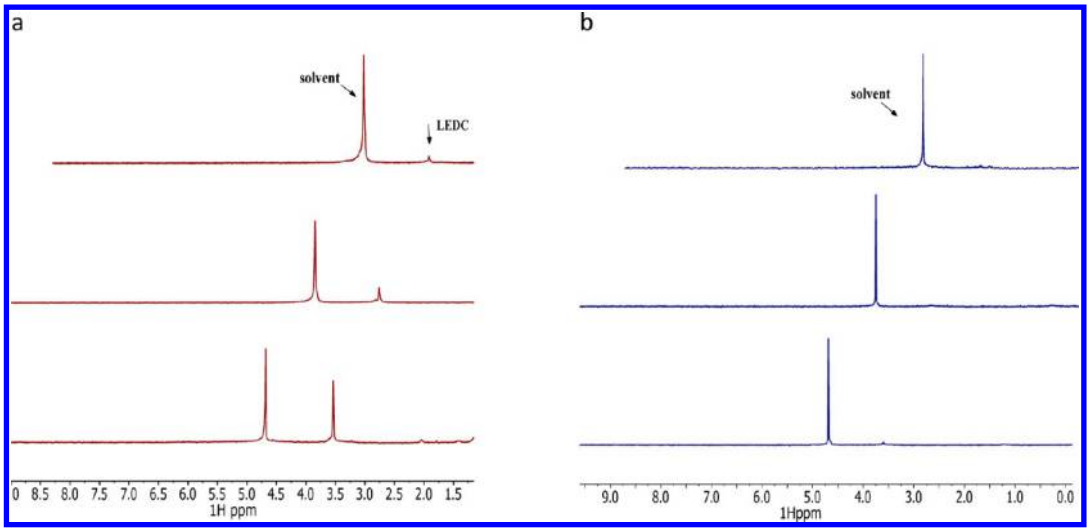

Figure 9. (a) ^{1}H NMR spectra of BF-Si electrode cycled in EC-electrolyte and exacted by D_2O from top: 1st cycle, 5th cycle, and 20th cycle. (b) ^{1}H NMR spectra of BF-Si electrode cycled in FEC-electrolyte and exacted by D_2O from top: 1st cycle, 5th cycle, and 20th cycle.

cm^{-1}, along with the appearance of a new absorption at 1810 cm^{-1}. The absorptions are very similar to those reported for polymeric decomposition product of FEC.[17] The IR spectra are different from those observed for the BF-Si anode cycled with $LiPF_6$/EC, supporting a change in the composition of the SEI. The intensity of the absorption characteristic of residual $LiPF_6$ (870 cm^{-1}) has greater intensity for the electrodes cycled with FEC than the electrodes cycled with EC, which is in agreement with the XPS data, as described above. This may be due to binding or trapping of the PF_6^- anions by polymeric decomposition product of FEC.

NMR Multinuclear Analysis of BF-Si Electrodes Extracted with D_2O. To further characterize the structure of the SEI on BF-Si anodes, ^{1}H, ^{13}C, ^{19}F, and ^{29}Si NMR spectroscopy of D_2O extracts of the BF-Si electrodes has been conducted. The ^{1}H NMR spectra of extracts of BF-Si electrodes cycled with $LiPF_6$/EC electrolyte contain a single peak at 3.51 ppm (s) consistent with lithium ethylene dicarbonate (LEDC) (Figure 9a).[31] LEDC is the only reduction product of EC observed on graphite electrodes, and thus the same reduction product of EC is observed on both silicon and graphite electrodes. The ^{13}C NMR spectrum contains a peak at 62.5 ppm, characteristic of LEDC.[20,32] However, unfortunately, because of the low concentration of the LEDC and the absence of hydrogen atoms directly attached to carbonyl carbon (lack of nuclear Overhauser effect) the resonance for the C═O is too weak to be observed. The intensity of the LEDC resonance continually increases with increased cycling, suggesting that the $LiPF_6$/EC electrolyte reduction continues and the BF-Si anode is not passivated during the first 20 cycles. The results are consistent with previous reports of continuous electrolyte reduction on Si electrodes due to the large volume changes. The lack of passivation is one of the most severe problems for Si electrodes and is the main contributor to poor cycling performance.[32] The ^{19}F NMR spectra of extracts of BF-Si electrodes cycled with $LiPF_6$/EC electrolyte contain peaks characteristic of residual $LiPF_6$ at −72.2 ppm (d) and a peak at −123 ppm (s), characteristic of LiF. The concentration of LiF increases with increasing cycle number, suggesting that both EC and $LiPF_6$ continue to be reduced throughout the cycling process (Figure 10). The ^{29}Si NMR spectra of the D_2O extracts contain no observable resonances, suggesting that either the silicon species are not soluble in water or the concentrations are below our detection limits.

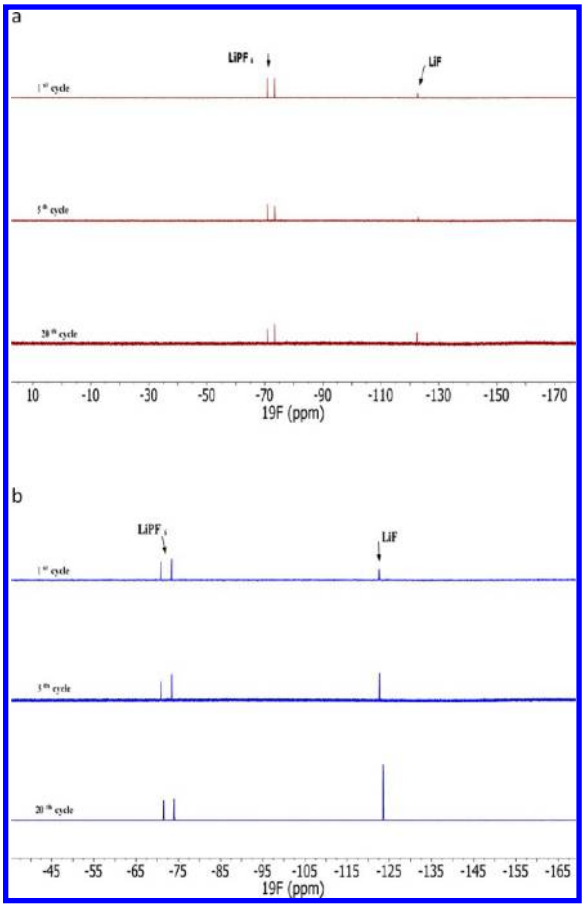

Figure 10. (a) ^{19}F NMR spectra of BF-Si electrode cycled in EC-electrolyte and exacted by D2O from top: 1st cycle, 5th cycle, and 20th cycle. (b) ^{19}F NMR spectra of BF-Si electrode cycled in FEC-electrolyte and exacted by D_2O from top: 1st cycle, 5th cycle, and 20th cycle.

The ^{1}H NMR spectra of D_2O extracts from BF-Si electrodes cycled with $LiPF_6$/FEC electrolyte contain no observable peaks even after 20 cycles (Figure 9b). The lack of any observable

dx.doi.org/10.1021/jp404155y | J. Phys. Chem. C 2013, 117, 13403−13412

peaks in the ^{1}H NMR spectra is consistent with the presence of an insoluble organic polymer on the BF-Si anode surface.[17,18] The ^{19}F NMR spectra of the BF-Si extracts contain peaks characteristic of residual $LiPF_6$ at −72.2 ppm (d) and a peak at −123 ppm (s), characteristic of LiF. The concentration of LiF increases with increasing cycle number. (Figure 10b) Moreover, the concentration of LiF is much greater for extracts of BF-Si electrodes cycled with $LiPF_6$/FEC than is observed for BF-Si electrodes cycled with $LiPF_6$/EC, suggesting that FEC may be an additional source of LiF. To confirm that FEC can be a source of LiF, BF-Si/Li cells were cycled with 1.2 M $LiClO_4$/FEC. Analysis of the D_2O extracts of BF-Si electrodes cycled (one cycle) with $LiClO_4$/FEC electrolyte by ^{19}F NMR spectroscopy reveal a single resonance at −123 ppm consistent with the presence of LiF (Figure 11). Thus the reduction

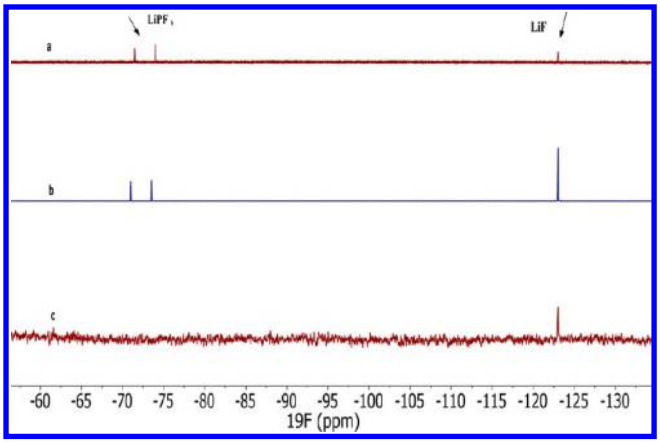

Figure 11. (a) ^{19}F NMR spectrum of BF-Si electrode cycled in EC-electrolyte after 20 cycles. (b) ^{19}F NMR spectrum of BF-Si electrode cycled in FEC-electrolyte after 20 cycles. (c)BF-Si electrodes cycled in 1.2 M $LiClO_4$/FEC electrolyte.

reaction of FEC generates LiF along with an unstable organic radical species, which is polymerized on the BF-Si electrodes (Scheme 1). The polymeric species has been proposed to be

Scheme 1

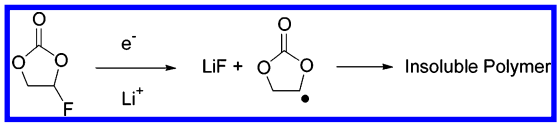

either a poly(alkene)[18] or a poly(carbonate).[17] However, because of the poly solubility of the polymerized organic material, characterization via solution NMR spectroscopy is not possible.

DISCUSSION

The SEI on BF-Si anodes was investigated for two different electrolytes, $LiPF_6$/EC and $LiPF_6$/FEC, via a combination of analytical techniques, TEM with EDX, solution NMR, XPS, and FT-IR. The SEI generated from $LiPF_6$/EC is thick and becomes integrated with the silicon nanoparticles after 20 cycles. The SEI is primarily composed of LEDC, LiF, and Li_xSiO_y but also contains low concentrations of Li_2CO_3 and $LiPF_6$. The concentrations of LEDC and LiF are high at the surface of the cycled particles, as detected via XPS (top ∼5 nm). The concentration of the bulk SEI, as determined by TEM/EDX, contains high concentrations of Si, C, and O and a low concentration of F, consistent with an inner SEI composed primarily of Li_xSiOy and LEDC. The IR spectra and D_2O extracts of the cycled BF-Si electrodes reveal that LEDC is the predominant organic component in the SEI. Thus the data are in qualitative agreement with the results of Edstrom and coworkers supporting an inner SEI primarily composed of Li_xSiO_y and LEDC and an outer SEI primarily composed of LEDC and LiF.[10,11] The layered SEI is different than the homogeneous SEI generated on BF graphite anodes. The differences are likely due to the differences in the nature of Li−Si alloying and lithium intercalation into graphite. However, the primary decomposition products of the electrolyte are the same, LEDC and LiF.

The SEI generated from $LiPF_6$/FEC after 20 cycles is quite different than the SEI generated from $LiPF_6$/EC. The SEI is primarily composed of LiF, Li_xSiO_y, and an insoluble organic polymer species but also contains low concentrations of $Li_xPF_yO_z$ and $LiPF_6$. The concentrations of LiF and the organic polymer are high at the surface of the cycled particles, as detected by XPS. However, the bulk SEI, as determined by TEM/EDX, has a much higher LiF content than that observed for the SEI generated from $LiPF_6$/EC. The Si concentration is lower (21.4%) and the concentrations of C, O, and F of the bulk SEI (EDX, 26.5, 18.6, and 32.8%, respectively) are similar to the surface SEI (XPS, 35.8, 29.5, and 29.4%, respectively). The TEM images also depict a clearer demarcation between the silicon nanoparticles and the SEI. This feature suggests that the SEI generated from $LiPF_6$/FEC is less layered and contains less Li_xSiO_y. The IR spectra reveal the presence of an organic polymer that likely contains some polycarbonate. The D_2O extractions reveal a high concentration of LiF but no soluble organic components. An SEI composed of a high concentration of LiF and an organic polymer leads to better capacity retention of BF-Si anodes, but it is not clear which component, the high concentration of LiF or the organic polymer, is more important to SEI stability and capacity retention.

CONCLUSIONS

The cycling performance of BF-Si electrodes with $LiPF_6$/EC and $LiPF_6$/FEC electrolytes was investigated. The surfaces of BF-Si electrodes were examined via a unique combination of TEM with EDX, solution NMR, SEM, XPS, and FT-IR to understand the differences in cycling performance. Ex situ TEM analysis suggests that there are significant changes to the silicon nanoparticles upon cycling. Electrodes cycled with $LiPF_6$/EC electrolyte have poor cycling performance. The BF-Si nanoparticles form a continuous amorphous phase with the SEI after 20 cycles. BF-Si electrodes cycled with $LiPF_6$/FEC have better capacity retention and clearer separation of the Si nanoparticle and the SEI. The composition of the SEI was characterized via NMR spectroscopy of the D_2O extracts of the BF-Si electrode. The primary components of the SEI formed with $LiPF_6$/EC electrolyte are LEDC, LiF, and Li_xSiO_y. The predominant products of SEI formed with $LiPF_6$/FEC electrolyte are LiF, an insoluble polymeric species, and Li_xSiO_y. The concentration of LiF is much higher for BF-Si electrodes cycled with $LiPF_6$/FEC than with $LiPF_6$/EC, and FEC is an additional source of LiF. The SEI formed with the $LiPF_6$/FEC electrolyte provides superior passivation of the BF-Si electrodes, leading to better capacity and structure retention.

dx.doi.org/10.1021/jp404155y | J. Phys. Chem. C 2013, 117, 13403−13412

AUTHOR INFORMATION

Notes

The authors declare no competing financial interest.

ACKNOWLEDGMENTS

We gratefully acknowledge funding from Department of Energy Office of Basic Energy Sciences EPSCoR Implementation award (DE-SC0007074).

REFERENCES

(1) Obrovac, M. N.; Christensen, L. Structural Changes in Silicon Anodes During Lithium Insertion/Extraction. *Electrochem. Solid State Lett.* **2004**, *7*, A93−A96.
(2) Chon, M. J.; Sethuraman, V. A.; McCormick, A.; Srinivasan, V.; Guduru, P. R. Real-Time Measurement of Stress and Damage Evolution During Initial Lithiation of Crystalline Silicon. *Phys. Rev. Lett.* **2011**, *107*, 045503.
(3) Benedek, R.; Thackeray, M. M. Lithium Reactions with Intermetallic-Compound Electrodes. *J. Power Sources* **2002**, *110*, 406−411.
(4) Ren, Y. R.; Ding, J. N.; Yuan, N. Y.; Jia, S. Y.; Qu, M. Z.; Yu, Z. L. Preparation and Characterization of Silicon Monoxide/Graphite/Carbon Nanotubes Composite as Anode for Lithium-Ion Batteries. *J. Solid State Electrochem.* **2012**, *16*, 1453−1460.
(5) Wu, H.; Cui, Y. Designing Nanostructured Si Anodes for High Energy Lithium Ion Batteries. *Nano Today* **2012**, *7*, 414−429.
(6) Aurbach, D. Review of Selected Electrode−Solution Interactions Which Determine the Performance of Li and Li Ion Batteries. *J. Power Sources* **2000**, *89*, 206−218.
(7) Verma, P.; Maire, P.; Novák, P. A Review of the Features and Analyses of the Solid Electrolyte Interphase in Li-Ion Batteries. *Electrochim. Acta* **2010**, *55*, 6332−6341.
(8) Li, S. Y.; Xu, X. L.; Shi, X. M.; Li, B. C.; Zhao, Y. Y.; Zhang, H. M.; Li, Y. L.; Zhao, W.; Cui, X. L.; Mao, L. P. Composition Analysis of the Solid Electrolyte Interphase Film on Carbon Electrode of Lithium-Ion Battery Based on Lithium Difluoro(Oxalate)Borate and Sulfolane. *J. Power Sources* **2012**, *217*, 503−508.
(9) Xu, K. Nonaqueous Liquid Electrolytes for Lithium-Based Rechargeable Batteries. *Chem. Rev.* **2004**, *104*, 4303−4418.
(10) Philippe, B.; Dedryvère, R.; Gorgoi, M.; Rensmo, H.; Gonbeau, D.; Edström, K. Role of the $LiPF_6$ Salt for the Long-Term Stability of Silicon Electrodes in Li-Ion Batteries − a Photoelectron Spectroscopy Study. *Chem. Mater.* **2013**, *25*, 394−404.
(11) Philippe, B.; Dedryvere, R.; Allouche, J.; Lindgren, F.; Gorgoi, M.; Rensmo, H.; Gonbeau, D.; Edstrom, K. Nanosilicon Electrodes for Lithium-Ion Batteries: Interfacial Mechanisms Studied by Hard and Soft X-Ray Photoelectron Spectroscopy. *Chem. Mater.* **2012**, *24*, 1107−1115.
(12) Arreaga-Salas, D. E.; Sra, A. K.; Roodenko, K.; Chabal, Y. J.; Hinkle, C. L. Progression of Solid Electrolyte Interphase Formation on Hydrogenated Amorphous Silicon Anodes for Lithium-Ion Batteries. *J. Phys. Chem. C* **2012**, *116*, 9072−9077.
(13) Trill, J. H.; Tao, C. Q.; Winter, M.; Passerini, S.; Eckert, H. NMR Investigations on the Lithiation and Delithiation of Nanosilicon-Based Anodes for Li-Ion Batteries. *J. Solid State Electrochem.* **2011**, *15*, 349−356.
(14) Elazari, R.; Salitra, G.; Gershinsky, G.; Garsuch, A.; Panchenko, A.; Aurbach, D. Li Ion Cells Comprising Lithiated Columnar Silicon Film Anodes, TiS_2 Cathodes and Fluoroethyene Carbonate (FEC) as a Critically Important Component. *J. Electrochem. Soc.* **2012**, *159*, A1440−A1445.
(15) Choi, N. S.; Yew, K. H.; Lee, K. Y.; Sung, M.; Kim, H.; Kim, S. S. Effect of Fluoroethylene Carbonate Additive on Interfacial Properties of Silicon Thin-Film Electrode. *J. Power Sources* **2006**, *161*, 1254−1259.
(16) Dalavi, S.; Guduru, P.; Lucht, B. L. Performance Enhancing Electrolyte Additives for Lithium Ion Batteries with Silicon Anodes. *J. Electrochem. Soc.* **2012**, *159*, A642−A646.
(17) Etacheri, V.; Haik, O.; Goffer, Y.; Roberts, G. A.; Stefan, I. C.; Fasching, R.; Aurbach, D. Effect of Fluoroethylene Carbonate (FEC) on the Performance and Surface Chemistry of Si-Nanowire Li-Ion Battery Anodes. *Langmuir* **2011**, *28*, 965−976.
(18) Nakai, H.; Kubota, T.; Kita, A.; Kawashima, A. Investigation of the Solid Electrolyte Interphase Formed by Fluoroethylene Carbonate on Si Electrodes. *J. Electrochem. Soc.* **2011**, *158*, A798−A801.
(19) Lin, Y. M.; Klavetter, K. C.; Abel, P. R.; Davy, N. C.; Snider, J. L.; Heller, A.; Mullins, C. B. High Performance Silicon Nanoparticle Anode in Fluoroethylene Carbonate-Based Electrolyte for Li-Ion Batteries. *Chem. Commun.* **2012**, *48*, 7268−7270.
(20) Nie, M.; Chalasani, D.; Abraham, D. P.; Chen, Y.; Bose, A.; Lucht, B. L. Lithium Ion Battery Graphite Solid Electrolyte Interphase Revealed by Microscopy and Spectroscopy. *J. Phys. Chem. C* **2013**, *117*, 1257−1267.
(21) Kang, S. H.; Abraham, D. P.; Xiao, A.; Lucht, B. L. Investigating the Solid Electrolyte Interphase Using Binder-Free Graphite Electrodes. *J. Power Sources* **2008**, *175*, 526−532.
(22) Xiao, A.; Yang, L.; Lucht, B. L.; Kang, S. H.; Abraham, D. P. Examining the Solid Electrolyte Interphase on Binder-Free Graphite Electrodes. *J. Electrochem. Soc.* **2009**, *156*, A318−A327.
(23) Benoit, R. X-Ray Photoelectron Spectroscopy. *Vide: Sci., Tech. Appl.* **2003**, *58*, 219−+.
(24) Ng, S.-H.; Wang, J.; Wexler, D.; Konstantinov, K.; Guo, Z.-P.; Liu, H.-K. Highly Reversible Lithium Storage in Spheroidal Carbon-Coated Silicon Nanocomposites as Anodes for Lithium-Ion Batteries. *Angew. Chem., Int. Ed.* **2006**, *45*, 6896−6899.
(25) Wen, Z. S.; Yang, J.; Wang, B. F.; Wang, K.; Liu, Y. High Capacity Silicon/Carbon Composite Anode Materials for Lithium Ion Batteries. *Electrochem. Commun.* **2003**, *5*, 165−168.
(26) Song, J. W.; Nguyen, C. C.; Song, S. W. Stabilized Cycling Performance of Silicon Oxide Anode in Ionic Liquid Electrolyte for Rechargeable Lithium Batteries. *RSC Adv.* **2012**, *2*, 2003−2009.
(27) Nguyen, C. C.; Song, S. W. Interfacial Structural Stabilization on Amorphous Silicon Anode for Improved Cycling Performance in Lithium-Ion Batteries. *Electrochim. Acta* **2010**, *55*, 3026−3033.
(28) Sethuraman, V. A.; Srinivasan, V.; Bower, A. F.; Guduru, P. R. In Situ Measurements of Stress-Potential Coupling in Lithiated Silicon. *J. Electrochem. Soc.* **2010**, *157*, A1253−A1261.
(29) Bettge, M.; Li, Y.; Sankaran, B.; Rago, N. D.; Spila, T.; Haasch, R. T.; Petrov, I.; Abraham, D. P. Improving High-Capacity Li1.2ni0.15mn0.55co0.1o2-Based Lithium-Ion Cells by Modifiying the Positive Electrode with Alumina. *J. Power Sources* **2013**, *233*, 346−357.
(30) Zhuang, G. R. V.; Xu, K.; Yang, H.; Jow, T. R.; Ross, P. N. Lithium Ethylene Dicarbonate Identified as the Primary Product of Chemical and Electrochemical Reduction of EC in 1.2 M $LiPF_6$/EC:EMC Electrolyte. *J. Phys. Chem. B* **2005**, *109*, 17567−17573.
(31) Xu, K.; Zhuang, G. R. V.; Allen, J. L.; Lee, U.; Zhang, S. S.; Ross, P. N.; Jow, T. R. Syntheses and Characterization of Lithium Alkyl Mono- and Dicarbonates as Components of Surface Films in Li-Lon Batteries. *J. Phys. Chem. B* **2006**, *110*, 7708−7719.
(32) Chan, C. K.; Ruffo, R.; Hong, S. S.; Cui, Y. Surface Chemistry and Morphology of the Solid Electrolyte Interphase on Silicon Nanowire Lithium-Ion Battery Anodes. *J. Power Sources* **2009**, *189*, 1132−1140.